ELSEVIER

Hydrophobicity and functionality maps of farnesyltransferase

Shaheen Ahmed, Nicolas Majeux, and Amedeo Caflisch

Department of Biochemistry, University of Zürich, Zürich, Switzerland

Farnesyltransferase (FTase) catalyzes the attachment of a 15-carbon isoprenoid moiety, farnesyl, through a thioether linkage to a cysteine near the C-terminus of oncogenic Ras proteins. These transform animal cells to a malignant phenotype when farnesylated. Hence, FTase is an interesting target for the development of antitumor agents. In this work we first investigate the active site of FTase by mapping its hydrophobic patches. Then the program SEED is used to dock functional groups into the active site by an exhaustive search and efficient evaluation of the binding energy with solvation. The electrostatic energy in SEED is based on the continuum dielectric approximation and consists of screened intermolecular energy and protein and fragment desolvation terms. The results are found to be consistent with the sequence variability of the tetrapeptide substrate. The distribution of functional groups (functionality maps) on the substrate binding site allows for identification of modifications of the tetrapeptide sequence that are consistent with potent peptidic inhibitors. Furthermore, the best minima of benzene match corresponding moieties of an inhibitor in clinical trials. The functionality maps are also used to design a library of disubstituted indoles that might prevent the binding of the protein substrates. © 2001 by Elsevier Science Inc.

Keywords: CaaX motif, tetrapeptide substrate, library docking, library of disubstituted indoles, SEED, CCLD

INTRODUCTION

Ras proteins play a critical role in signal transduction pathways that control cell growth and differentiation. Mutants of three human Ras proteins (Ha-Ras, Ki-Ras and N-Ras) are found in 20–30% of all human cancers,[1–3] which makes them an attractive target for antitumoral drug design. A promising approach for interfering in the Ras function involves inhibition of the enzyme farnesyltransferase (FTase). This enzyme covalently links the isoprenoid moiety of farnesyl pyrophosphate (FPP) to the C-terminal part of Ras as well as to other membrane associated proteins.[4–6] This, among other fast posttranslational modifications, is required for their attachment to the plasma membrane, which is essential for their biological activity.[7–9] Ras processing and membrane association are signaled by a carboxyterminal tetrapeptide sequence present on all Ras proteins. This sequence is normally referred to as the CaaX motif, where 'C' stands for a cysteine, 'a' is generally an aliphatic amino acid, and 'X' is typically a methionine and, less frequently, a Ser, Ala, Phe, and Leu.[10] Although several FTase inhibitors are currently in clinical trials, there is a need for the design of novel, more selective, FTase inhibitors to lower toxic side effects. These include myelosuppression, diarrhea, and thrombocytopenia, which have been observed in phase I clinical trials.[11–15]

FTase is a heterodimeric zinc metalloenzyme. The zinc atom is coordinated by a cysteine, an aspartic acid, and a histidine, and is essential for the catalytic activity of FTase. Steady-state analysis[16] suggests that the reaction proceeds in a functionally ordered manner where the FPP substrate binds first to form a binary complex, followed by the binding of the CaaX motif. The rate-limiting step of this reaction seems to be the release of the prenylated product.[16] Prenylation only occurs when the tetrapeptide binds to the FTase after FPP has bound.[16] Binding of the CaaX peptide before FPP leads to a non-functional complex.[17] Because of the high intracellular concentration of FPP (approximately 1 μmol/L) it is assumed that most of the FTase in the cell is complexed with FPP.[18] As FTase has two substrates, there have been several approaches to develop either FPP-like, CaaX-like, or bisubstrate inhibitors to hinder Ras processing.[18,19]

In this article, we first characterize the active site of FTase, namely its overall hydrophobic and hydrophilic properties. Many programs are available to efficiently dock libraries of molecular fragments into a rigid protein binding site. Most of them use either a scoring function with a crude approximation of solvation[20–22] or a vacuum energy derived from a molecular mechanics force field.[23–25] The program SEED is used here because its binding energy is based on a comprehensive treatment of the electrostatic contribution, which includes an accurate evaluation of solvation effects within the dielectric con-

Color Plates for this article are on pages 380–387.

Corresponding author: Amedeo Caflisch, Department of Biochemistry, Winterthurerstrasse 190, CH 8057 Zürich, Switzerland. Tel.: (41 1) 635 55 21; fax: (41 1) 635 57 12.

E-mail address: caflisch@bioc.unizh.ch

Journal of Molecular Graphics and Modelling 19, 307–317, 2001

655 Avenue of the Americas, New York, NY 10010

1093-3263/01/$–see front matter
PIIS1093-3263(00)00075-9

tinuum approximation.[26] Although it is very difficult to predict toxic side effects, the molecular fragments docked by SEED are found frequently in the database of known drugs;[27] hence, they are probably less toxic than randomly selected fragments. The functionality maps of the FTase tetrapeptide binding site generated with SEED are analyzed by comparison with known peptidic ligands. The maps are then used to suggest possible modifications of the CaaX motif that might increase the affinity of peptidic or peptidomimetic inhibitors. Finally, a program for combinatorial ligand design (CCLD)[28] is used to generate a library of disubstituted indoles as potential competitive inhibitors of the peptide substrate. Indole was chosen as a scaffold because it is present in at least twelve known drugs,[27] which indicates that indole derivatives should have good pharmacological profiles. Furthermore, it is possible to synthesize polysubstituted indoles on a solid phase by a combinatorial approach.[29,30]

METHODS

The choice of the FTase conformation, the binding site definition, and the preparation of the system are presented first. Then a short description is given of the program SEED[26] and the combinatorial ligand design program CCLD.[28]

System Set-up

The 2.5 Å resolution X-ray structure of rat FTase complexed with an FPP analog, α-hydroxyfarnesylphosphonic-acid (αHFP), and the peptide CVIM[31] was downloaded from the Brookhaven PDB database[32] (access code 1QBQ). The crystal structures of the unliganded FTase[33] (access code 1FT1, 2.25 Å resolution) and the FTase complexed with FPP[34] (access code 1FT2, 3.4 Å resolution) were also used to analyze the effect of side chain displacement on the hydrophobicity of the active site. Hereafter, the structures will be named unliganded FTase (1FT1), binary complex (1FT2), and ternary complex (1QBQ). Visual analysis with the program WITNOTP (A. Widmer, unpublished) reveals displacement of the Met193β and Arg202β side chains as the main difference between the unliganded FTase and the binary complex. In the ternary complex a further displacement of Arg202β can be observed as well as rotations of the side chains of Tyr166α and Glu198β when compared with the binary structure. The positions of the remaining residues of the active site in the three structures of FTase do not differ considerably.

Since electrostatic interactions are long-ranged, it is more appropriate to run SEED/CCLD with FPP (total charge of -3) in the active site rather than αHFP (total charge of -2). The use of αHFP instead of FPP would lead to a different electrostatic potential in the FTase binding site. Hence, the αHFP was removed and the FPP structure was positioned into the FTase structure of the ternary complex by overlapping the binary and ternary complexes. In this way, no steric clashes were found between FPP and FTase.

Only 13 of the 284 water molecules of the ternary complex were kept. These are positioned in a cavity surrounded by Tyr166α, His170α, His201α, Gln207α, and Glu198β, whose center is at $\sim$15 Å from the nearest atom of the peptide. The cavity is not accessible from the peptide binding site because of the narrow path between Tyr166α and Tyr251α, which form the entrance to the cavity.

Hydrogen atoms were built with the HBUILD[35] option of the CHARMM program[36] and then minimized with rigid heavy atoms to a RMS of the energy gradient of 0.02 kcal/mol Å using the CHARMm22 force field (Molecular Simulations Inc. San Diego, CA USA).

Hydrophobicity Maps

The propensity of nonpolar groups to bind at the surface of a protein can be estimated and graphically displayed with the hydrophobicity maps.[37–39] For a set of five protein–protein complexes and five protein–ligand complexes, it was shown that the approaches based on the analysis of the surface curvature and/or the electrostatic potential are not always able to clearly distinguish regions where nonpolar and polar groups can bind.[39] The approach used in this study includes electrostatic desolvation, which enables easy discrimination between the hydrophobic and hydrophilic surface regions that are close in space. Briefly, the binding energy of a nonpolar probe sphere is evaluated as the sum of van der Waals interaction plus protein electrostatic desolvation in the continuum approximation.[39,40] The color rendering of the binding energy values on the protein surface allows one to distinguish hydrophilic from hydrophobic zones. The latter are used by the program SEED to direct the docking of apolar fragments.

Solvation Energy for Exhaustive Docking (SEED)

The program SEED determines favorable positions and orientations of rigid molecular fragments on the binding site surface of a receptor of known three-dimensional structure.[26] The receptor in this article is the FTase structure with FPP. The FTase structure was kept rigid in the X-ray conformation of the ternary complex.[31] The binding site for the SEED calculations was defined by the residues listed in the caption of Figure 1. A library of sixty-five fragments was used in this study. It contains 15 apolar, 38 polar neutral, and 12 charged fragments to map both the hydrophilic and hydrophobic regions of the peptide substrate binding site. For fragments with multiple discrete conformations, all of the conformers were docked, e.g., the cis and trans conformations of 2-butene.

Fragments of mainly hydrophilic character are docked such that at least one hydrogen bond between the receptor and the fragment is formed with close to optimal geometry. For this task, vectors on polar groups of both protein and fragments are defined automatically by SEED. For the zinc atom, a vector was defined from the zinc coordinates to the sulfur atom of the cysteine of the peptide substrate. This atom is located at the same position as the oxygen of the water molecule, which coordinates the zinc in the unliganded structure. Nonpolar fragments are docked in hydrophobic regions of the receptor, which are determined as described in the previous subsection. An approximated binding free energy for each fragment/receptor complex is evaluated as:

$$\Delta G_{binding} = \Delta G_{vdW} + \Delta G_{intermol.\ elect.} + \Delta G_{recept.\ desolv.\ elect.} + \Delta G_{frag.\ desolv.\ elect.} \quad (1)$$

The first two terms on the right side of the equation represent the fragment/receptor van der Waals interaction (ΔG_{vdW}) and the intermolecular electrostatic interaction ($\Delta G_{intermol.\ elect.}$) with solvent screening. $\Delta G_{recept.desolv.elect.}$ is the partial desol-

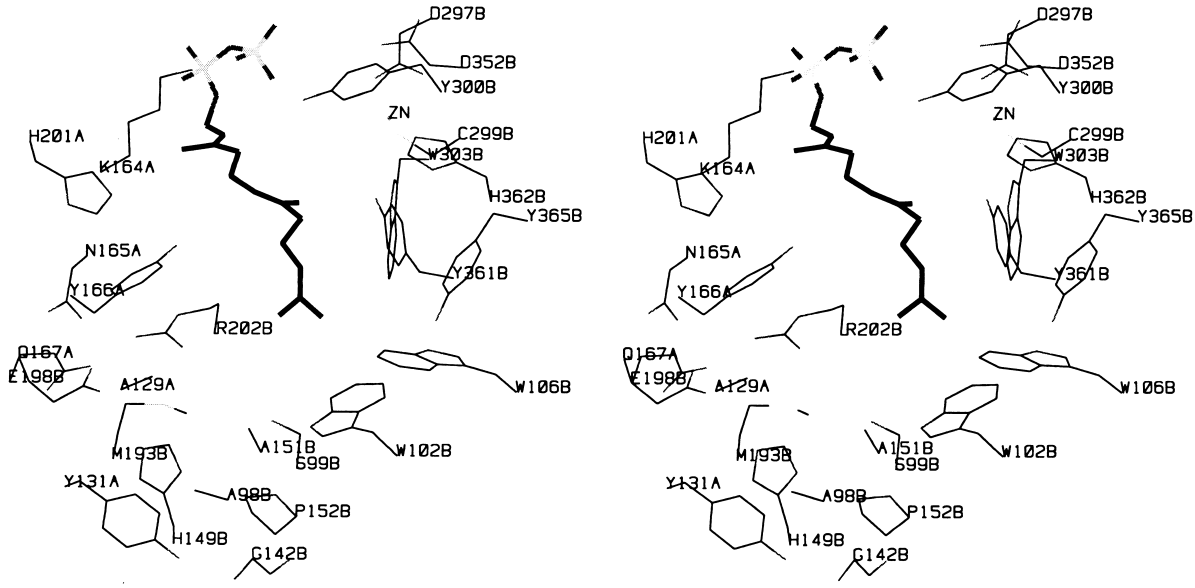

Figure 1. Stereoviews (wall eye) of the FTase binding site residues used in SEED. FPP is shown in thick lines. The twenty-six residues used as binding site in SEED/CCLD are labeled at their C_α. They are: Ala129α, Tyr131α, Lys164α, Asn165α, Tyr166α, Gln167α, His201α, Ala98β, Ser99β, Trp102β, Trp106β, Gly142β, His149β, Ala151β, Pro152β, Met193β, Glu198β, Arg202β, Asp297β, Cys299β, Tyr300β, Trp303β, Asp352β, Tyr361β, His362β, Tyr365β, and the Zn^{2+} atom.

vation of the receptor due to the displacement of the solvent by the fragment volume, while $\Delta G_{frag.\ desolv.\ elect.}$ is the partial desolvation of the fragment due to the receptor volume. Both desolvation terms are calculated in the continuum approximation.[26,40] To be consistent with the CHARMM parameterization of the partial charges, an interior dielectric value of 1.0 is employed for the volume enclosed by the solute, while the remaining volume is assigned a value of 78.5, corresponding to the dielectric constant of water at room temperature. In the present application of SEED, we used the same input parameters that were used in the original paper, except for the following three values: the number of apolar points on the receptor surface was increased to 200 (compared with 100 points for the thrombin application)[26] because of the large hydrophobic surface of the FTase binding site; the number of rigid body rotations of the fragment around each alignment vector was set to 72 (compared with 36); and the maximal angular deviation from the ideal hydrogen bond geometry was increased to 75° (compared with 50°) to sample more positions. Additional details about SEED (e.g., the clustering procedure) and a complete description of the continuum electrostatic method have been presented in previous publications.[26,40,41]

Computational Combinatorial Ligand Design (CCLD)

The aim of the CCLD program[28] is to combinatorially connect the molecular fragments docked by SEED to form candidate ligands. The linker units are small (not more than 3 covalent bonds) in order not to add considerably to the molecular weight. The user can specify in CCLD the minimal and maximal values for the distance (d) between linkage atoms for each connection type and the tolerance of the dihedral angles t1 for Csp3-Csp3 bonds (minima at +60, −60, 180°) and the dihedral angles t2 for Csp2-Csp3 bonds (minima at −90, +90°). In the present study the following values (in Å) were employed: $d < 0.40$, 0-bond; $1.4 < d < 1.6$, 1-bond; $2.2 < d < 2.8$, 2-bond; $3.2 < d < 4.5$, 3-bond. The tolerances for t1 and t2 were set to 40°, which yields the following allowed ranges for Csp3-Csp3 dihedrals: $20 < t1 < 100$, $-100 < t1 < -20$, $140 < t1 < 180$ and $-180 < t1 < -140$. The ranges allowed for Csp2-Csp3 dihedrals are: $-130 < t2 < -50$ and $50 < t2 < 130$. To limit the molecular weight of the candidate ligands, the maximal number of heavy atoms of each CCLD hit was restricted to forty.

The indole that serves as central skeleton for library design was placed manually in the center of the binding site with an orientation that allows its 1- and 5-substituents to reach the binding pocket containing the substrate side chains Val and Met, respectively. This indole was then automatically replicated 14 times by CCLD by 0.5 Å rigid body translations from its original position along the x-, y-, and z-axes (six replicas), and in the directions of the center of each octant (eight replicas). CCLD allows the user to specify which atoms have to be substituted; three linkage points were defined to obtain 1-, 3-, and 5-substituted indolic ligands. All of the sixty-five fragments in the SEED library were used by CCLD to generate candidate ligands. For each fragment type, the 70 positions with the best $\Delta G_{binding}$ were employed for a total of 4,550 fragments. The SEED run took 24 h and the CCLD run needed 18 h on a 195-MHz R10'000 processor.

RESULTS AND DISCUSSION

Hydrophobicity Maps of the FTase Active Site

The active site in the binary and ternary complexes is much more hydrophobic than in the unliganded structure (Color Plate

1). This is due to the rearrangement of Arg202β, whose side chain moves away from the FPP binding site and, in the binary complex, forms a bidentate ion pair with Asp200β. This displacement enables the FPP substrate to bind. SEED was used to dock propane, an apolar probe, into the unliganded FTase as well as into the FTase structure from the binary complex. The propane with the best free energy of binding lies in both cases $<$1 Å away from the terminal carbon atoms of the farnesyl moiety of FPP (Color Plate 2). While in the unliganded FTase structure, the propane representatives are mainly distributed over the tetrapeptide binding site, they cover a large part of the FPP binding site. The different distributions of propane in the two FTase structures clearly indicate the alteration of the FTase surface in its propensity to bind nonpolar fragments. The binding of FPP to FTase is an example of induced fit where the hydrophobic moiety of FPP shapes an apolar region on the protein surface by displacing the side chain of Arg202β.

The conformational changes between the FTase structure of the binary and the ternary complex are less pronounced. The active site of the ternary complex is slightly more hydrophilic than the one of the binary complex because of the different orientations of the Tyr166α, Glu198β, and Arg202β side chains. The displacement of Arg202β and the Tyr166α rotation of $\sim$100° around χ_1 are important for the variability of the CaaX motif, as explained in the next section.

FTase Functionality Maps

For the analysis of the FTase binding site, the SEED library consisted of general organic compounds and functional groups of amino acid side chains. The latter are useful for a comparison with the CaaX motif. The functionality maps of three nonpolar, two polar neutral, one negatively and one positively charged fragments are discussed in this section to illustrate the properties of the peptide binding site. Hereafter, the second and third positions of the CaaX motif will be named a1 and a2, respectively. SEED cluster representatives[26] will be called representatives or positions.

Hydrophobic Fragments SEED was used to dock 15 fragments without any hydrogen bond donors or acceptors and ranging in size from 2 heavy atoms (ethane) to 14 heavy atoms (dibenzocyclohexane). Furthermore, fragments with one or two hydrogen bonding groups but mainly hydrophobic character (e.g., diphenylether) were docked using the apolar vectors in the hydrophobic regions. Only the functionality maps of propane, benzene, and 5-phenyl-1,4-benzodiazepine-2-one (called 1,4-benzodiazepine hereafter) are analyzed in detail. Propane is small enough to give a detailed description of eventual small cavities. Benzene is the most common fragment in known drugs.[27] 1,4-Benzodiazepine is used to determine the binding modes of a series of known FTase inhibitors with 1,4-benzodiazepine as scaffold.[42] It was docked using the apolar vectors[26] because it is mainly hydrophobic, although it contains two hydrogen bonding groups. For comparison with the peptide substrate preferences, benzene is a good representative of the Phe side chain while propane describes the Val, Leu, Ile, and approximately the Cys, Pro, and Met side chains. The energy values and positions of the five propanes, benzenes, and 1,4-benzodiazepines with the lowest free energy of binding are listed in Table 1. The favorable van der Waals interaction contributes the most to the binding energy. The remaining apolar compounds show similar functionality maps, although the rank ordering is somewhat different depending on the fragment size.

Propane. Positions 1, 2 and 5 overlap the thiomethyl group of the Met side chain of the tetrapeptide (Color Plate 3a). There are two reasons for the strong preference of propane for the Met side chain pocket compared to benzene. First, the protein desolvation effects are smaller for propane than for benzene because of the different size of these fragments. Second, the Met side chain lies in a narrow pocket that is better accessible to propane than benzene. Propane 3 overlaps the side chain of Ile (a2) while the position of propane 4 indicates that Ile can be replaced by a larger hydrophobic side chain. The best propane close to the Val (a1) side chain has a rank of 15 and $\Delta G_{binding}$ of -0.5 kcal/mol compared to -5.8 kcal/mol for propane 1. This indicates that the a1 position of the CaaX motif is not favorable for apolar residues which is further supported by the SEED results for polar fragments. This is also consistent with the different orientation of the Val side chain in the absence of zinc.[43] It is likely that the zinc ion influences the position of the Ca_1 moiety of the substrate and that there is some strain in the binding mode of the a1 residue.

Benzene. Benzene 1 is in van der Waals contact with Trp106β and Tyr361β. It is situated on the Ile side chain of the CaaX motif, which indicates that the corresponding pocket is large enough for a Phe residue at position a2 (Color Plate 3b). Phe is not found at a2 of natural CaaX motifs but can inhibit FTase at very low concentrations (see also Table 2). Representative 2 is in edge-to-edge contact with Trp106β. Benzene 3 is close to the position of the Val (a1) side chain of the peptide substrate. Benzene 4, which interacts with Leu96β and Trp106β, also supports a Phe at a2. Benzene 5 overlaps the Met side chain of the tetrapeptide and interacts with Tyr131α and Trp102β. It has a significantly larger FTase desolvation penalty than the first four clusters. This is mainly due to the partial desolvation of the OH-group of Ser99β and the side chain of Gln167α.

Recently, several X-ray structures of FTase complexed with tricyclic inhibitors were published by Strickland et al.[44] One of these inhibitors, SCH 66336, is currently in clinical trials.[12] The SEED benzene positions with the best and third best free energy of binding match the left and right rings of the tricyclic system (Color Plate 3c). Considering the flexibility of FTase, this is a striking result because it was obtained with a FTase conformation originally complexed with αHFP and a tetrapeptide substrate. The remaining parts of SCH 66336 exhibit only weak interactions with the protein and are partially exposed to the solvent.[44]

1,4-Benzodiazepine. The 5-phenyl substituent of the 1,4-benzodiazepine position with the best energy makes strong interactions with the hydrophobic moiety of FPP while its bicyclic system interacts mainly with the side chains of Ala129α, and Leu96β (not shown). 1,4-Benzodiazepines 2 and 4 interact through their bicyclic rings with FPP and their benzene ring is exposed to the solvent similar to the valine side chain of the tetrapeptide. 1,4-Benzodiazepine 3 partly mimics the binding mode of Val and Ile of the CaaX motif while position 5 is close to the Ile and Met of the CaaX motif. The functionality map of 1,4-benzodiazepine is particularly interesting as it gives some hints on the binding mode of the FTase

Table 1. SEED functionality maps of the FTase-FPP complex

Rank[a]	Intermolecular		Electrostatic desolvation		$\Delta G^{b}_{binding}$	Site[c] and H-Bond partners[d]
	vdWaals	Elect	Receptor	Fragment		
Hydrophobic groups						
Propane						
1	−10.6	0.5	4.2	0.0	−5.8	M
2	−10.4	0.1	5.8	0.0	−4.5	M
3	−6.4	0.6	1.3	0.0	−4.5	I
4	−7.2	0.1	3.1	0.1	−3.9	Leu96β, Trp106β
5	−9.3	0.1	5.4	0.0	−3.7	M
Benzene						
1	−6.8	0.4	2.4	1.2	−2.9	I; Trp102β, Trp106β, Tyr361β
2	−5.4	0.5	1.1	1.2	−2.6	Leu96β, Trp106β, Tyr361β
3	−6.7	−0.1	3.1	1.1	−2.5	V; FPP
4	−7.3	−0.3	3.9	1.3	−2.4	Leu96β, Trp106β
5	−11.6	0.2	7.9	1.1	−2.4	M; Trp102β, Tyr131α, Ser99β
5-Phenyl-1,4-benzodiazepine-2-one						
1	−15.8	−3.2	10.5	2.3	−6.3	FPP, Leu96β, Ala129α
2	−15.2	−1.7	8.8	2.1	−6.0	FPP, Ala129α, Tyr166α
3	−15.9	−1.9	10.0	2.2	−5.6	V,I; Ala129α, Tyr166α, Trp102β
4	−14.5	−0.1	7.1	2.1	−5.3	FPP, Tyr166α, Ala129α
5	−22.1	0.5	14.0	2.3	−5.3	I,M; Trp102β, Tyr131α, Ser99β
Polar groups						
Phenol						
1	−5.7	−7.6	3.4	3.0	−7.0	V; Lys164αCO
2	−5.1	−8.4	3.3	3.4	−6.8	V; Lys164αCO
3	−6.1	−8.5	5.1	3.9	−5.7	I; Arg202βN$^{\zeta}$
4	−5.9	−8.6	5.6	3.9	−5.0	M; Tyr166αNH, Asn165αN$^{\delta 2}$
5	−3.0	−8.3	4.5	3.1	−3.8	V; Lys164αCO
Imidazole						
1	−9.4	−2.4	4.6	2.7	−4.6	M; Ser99βOH, Ala98βCO
2	−5.7	−3.3	2.4	2.3	−4.3	V; Lys164αCO
3	−8.6	−3.1	5.6	2.6	−3.4	M; Ala98βCO, Ser99βOH
4	−9.2	−2.9	6.3	2.7	−3.2	M; Ala98βCO
5	−4.9	−3.3	2.8	2.4	−2.9	V; Lys164αCO
Charged groups						
Methyl-ammonium						
1	−3.2	−68.3	21.9	42.3	−7.3	PP[e]; Asp297βO$^{\delta 2}$
2	−3.2	−16.5	2.6	21.4	4.3	V; Lys164αCO
Acetate						
1	−1.7	−11.1	7.8	11.3	6.3	Lys164αN$^{\zeta}$

All energy values are in kcal/mol.
[a] Ranked among the positions of the same fragment type according to total binding energy.
[b] Sum of the values of the preceding four columns, i.e., intermolecular and electrostatic desolvation energies.
[c] Sites occupied by the tetrapeptide substrate (NH2-Cys-Val-Ile-Met-COOH) are defined by the one-letter code, while interactions with FTase and/or FPP are defined by the three-letter code.
[d] For positions with more than one H-bond partner, the first H-bond partner in the list is the one that was used by SEED for docking.
[e] Pyrophosphate moiety of FPP.

Table 2. Variability and possible modifications of the CaaX motif

	C	a_1	a_2	X
Mammalian and *S. cerevisiae* sequences[a]	Cys	Val	Val	Met
		Ile	Ile	Leu
		Ala	Leu	Ser
		Cys		*Ala*
		Ser		*Cys*
Tetrapeptides of Reiss et al.[b49]		Leu	Thr	Phe
		Phe	Ser	Val
		Lys	Pro	Pro
		Glu	Ala	Ile
		Gly		
		Pro		
Tetrapeptide inhibitors of Goldstein et al.[54]	Pen[c]		Phe	
			Tyr	
			Trp	
SEED results[d]				
propane		−0.5	−4.5	−5.8
benzene		1.2	−2.9	−2.4
phenol		−3.8	−2.1	0.3
indole		−3.1	3.8	0.2
imidazole		−2.9	−1.0	−4.6
methanol		−2.6	−2.1	−2.2
amide		−10.0	—	−6.0
Sequences proposed on the basis of SEED maps[e]		Tyr	Phe	Val
		Trp	Tyr	Ile
		His	Thr	Phe
		Thr	His	His
		Asn		Thr
		Gln		Asn
				Gln

[a] COOH-terminal tetrapeptide sequences.[1,17,51–53] Residues in italics appear only in *S. cerevisiae.*
[b] Only residues not listed in the first row and with IC_{50} values <10 μM are given. They are ordered according to IC_{50} values.
[c] L. penicillamine.
[d] The values listed are the most favorable binding energy at the corresponding position in kcal/mol.
[e] Only residues not found in the mammalian and *S. cerevisiae* sequences are given.

inhibitors proposed by James et al.[42] In their series of 1,4-benzodiazepine inhibitors, the C-3 atom is substituted by a Cys and the N-1 atom by either a Ser, Leu, or Met. The compound with the Met substituent yielded the best inhibitory activity of the ten compounds tested.[42] The SEED results strongly suggest that these inhibitors bind in an extended conformation similar to that of the CaaX motif. The cysteine of the inhibitor coordinates the zinc. The seven-membered ring of the bicyclic system of the 1,4-benzodiazepine overlaps the backbone of the Val (a1) residue while the six-membered ring interacts with Trp106α and Tyr361α (usually in contact with the a2 residue). The 5-phenyl substituent is exposed to the solvent. The methionine of the inhibitor fills the same narrow pocket as the corresponding side chain of the tetrapeptide substrate.

Polar Fragments The polar neutral groups of the SEED library are distributed over the hydrophilic regions of the FTase binding site. The functional groups of the Tyr (phenol) and His (imidazole) side chains are discussed in details. The other polar fragments showed analogous distribution patterns.

Phenol. Representatives 1, 2, and 5 act as hydrogen bond donors to the main chain CO of Lys164α and overlap the Val (a1) side chain of the tetrapeptide substrate (Color Plate 4a, Table 1). This suggests that a polar side chain (i.e., threonine or tyrosine) at position a1 might increase the affinity of CaaX-mimicking inhibitors towards FTase. The benzene ring of phenol 3 is close to the Ile (a2) residue of the tetrapeptide and its OH-group accepts a hydrogen bond from the N^{ζ} atom of Arg202β. Phenol 4 acts as a hydrogen bond acceptor for the NH_2 group of the Asn165α side chain.

Imidazole. Imidazoles 1, 3, and 4 (Color Plate 4b) overlap the Met side chain of the tetrapeptide. They donate a hydrogen bond to the OH-group of Ser99β or to the main chain CO of Ala98β. The desolvation penalty of the receptor at this position is more than two times higher than for imidazoles 2 and 5 (as already noticed for benzene). The van der Waals energies for positions 1, 3, and 4 are more favorable than for positions 2 and 5 because the pocket containing the Met side chain is more concave than the one of the Val. Both the apolar and polar fragments at this position pay a considerably large penalty of desolvation but their van der Waals energy is very favorable.

Charged Fragments Eight of the 12 charged fragments docked by SEED have an unfavorable, i.e., positive free energy of binding mainly due to fragment and protein desolvation. The four fragments with $\Delta G_{binding} < 0$ are benzamidine, methyl-amidine, methyl-ammonium, and methyl-guanidinium. The methyl-ammonium representative with the most favorable $\Delta G_{binding}$ contacts the pyrophosphate moiety of FPP (see below), while the best benzamidine, methyl-amidine, and methyl-guanidinium form a hydrogen bond with the main chain CO of Lys164α. For mapping the peptide substrate binding site, the functional groups of the Lys side chain (methyl-ammonium), and Asp and Glu side chains (acetate) are discussed.

Methyl-ammonium. Of all positions of methyl-ammonium, only representative 1 has a favorable free energy of binding (Table 1). It interacts with the pyrophosphate group of FPP in accord with the experimentally determined position of a manganese ion.[43] The desolvation of the receptor is high but is compensated by a very good electrostatic interaction energy. Methyl-ammonium 2 to 5 interact with the main chain CO of Lys164α. As this position is less buried in the receptor than that of representative 1, the desolvation of the fragment is considerably reduced. Yet, methyl-ammonium 2 to 5 have an unfavorable $\Delta G_{binding}$ because the desolvation penalty is not compensated by the intermolecular interactions, which are screened by the solvent (Table 1).

Acetate. None of the positions of acetate has a negative total free energy of binding (Table 1). The first 5 clusters interact with Lys164αN^{ζ}. The acetate closest to the carboxy terminus of the CVIM substrate has a rank of 65 and an unfavorable binding energy. In the crystal structure of the ternary complex a water molecule bridges the carboxy terminus of the peptide substrate to the side chains of His149β, Glu198β, and Arg202β.[31] This water molecule was not taken into account in the SEED docking.

Comparison with Experimental Data on Peptidic Substrates and Inhibitors

In the last decade, several studies on the substrate specificity of FTase have been published.[45–50] Reiss et al.[49] used a positional scanning approach to mutate the Cys-Val-Ile-Met substrate independently at the three positions downstream of the cysteine. This yielded a wide variety of tetrapeptide sequences. These CaaX-derived motifs were then tested for their ability to compete with $p21^{Ha\text{-}ras}$ for acceptance of a farnesyl group. In a recent study, Boutin et al.[50] synthesized a tetrapeptide library on solid phase. The tetrapeptides were tested for their ability to serve as substrate for farnesylation by measuring the consumption of [^{3}H]farnesyl pyrophosphate. The main difference between the results of Reiss et al. and Boutin et al. is that Gln was found to be favorable at a2 by the latter. The slightly different conclusions of the two groups about the substrate specificity of FTase indicate that some mutations of the CaaX motif at one position might be incompatible with a simultaneous mutation at another position of the CaaX motif.

The results of the present computational study can be used to suggest modifications of the CVIM motif that might improve the binding affinity of peptidic CaaX-like inhibitors. The SEED results indicate that a polar residue (Thr, Tyr, Asn, or Gln) is favored at the a1 position, which is consistent with the data of Boutin et al.[50] In the crystal structure of the ternary complex, the Val (a1) residue of the tetrapeptide is exposed to the solvent and the environment in this part of the FTase binding site is rather hydrophilic, which is mainly due to the main chain carbonyl group of Lys164α. Furthermore, a recent crystal structure of FTase complexed with the C-terminal amino acid sequence of K-Ras4B suggests that inhibitory tetrapeptides could bind by adopting a β-turn conformation with a completely different orientation of the Val (a1) side chain if the FTase is depleted of the zinc that was shown to be unnecessary for stability.[43]

The functionality maps show a clear preference for hydrophobic residues at the a2 position. This is in agreement with experimental data.[43,49,54] The benzene and phenol groups are also well accomodated in a2, in accord with known inhibitors containing Phe or Tyr at a2.[54] Goldstein et al.[54] have shown that CaaX tetrapeptides that contain an aromatic residue at the a2 position are not farnesylated and act as true inhibitors.

The SEED results for apolar and polar fragments suggest that the last residue of the CaaX motif can be either hydrophobic or hydrophilic. The natural substrates usually prefer a Met side chain, while mutational studies found that Ser and Gln can be accommodated as well.[49,50] The values of the intermolecular van der Waals interactions and the desolvation energies of the receptor at the position X are comparable for apolar and polar fragments (Table 1).

Library of Indolic FTase Inhibitors

Several known drugs contain an indole or an indole derivative as scaffold.[27] Moreover, it has been shown that polysubstituted indoles can be synthesized combinatorially on the solid phase.[29,30] To generate indolic candidate ligands, CCLD was applied on the SEED maps of the 65-fragment library. The indole was docked manually. This is necessary because SEED was developed to obtain favorable interactions of a small fragment with the binding site of a protein. Central skeletons, in contrast, usually do not exhibit strong interactions with the protein but only their substituents do. In the crystal structures of the ternary complex, only two groups of the tetrapeptide backbone are hydrogen bonded to FTase: the CO of Ile (a2) acts as acceptor for the side chain of Arg202β and the C-terminal carboxy accepts from the amid group of the side chain of Gln167α.[31,43] Hence, the indole can be used to replace the peptide main chain without a significant loss in binding affinity. The set-up of the CCLD run was performed as outlined in the Methods section. This led to 754 1,5-disubstituted indoles. From these results, a library of possible substituents was derived by considering the fragments which show the most favorable interactions with the protein (Figure 2). Many of these compounds can be synthesized by a combinatorial approach and for those that are not accessible, close analogs with slightly modified substituents can be synthesized.[30] The candidate ligands fill the Met binding pocket with the C-5 substituent and the region occupied by the Val side chain with the substituent at N-1 (Color Plate 5). Nothing larger than a methyl group is allowed at C-3, because this part of the indole is close to the protein, namely to residues Tyr166α and Arg202β. Two CHARMm22 minimizations, one within the rigid protein and one for the isolated ligand, were performed on each member of the indolic library and the VIM peptide to determine the intermolecular energy and the strain of the candidate ligands upon binding to the FTase. No major displacement could be observed upon minimization and the hydrogen bonds between the substituents and FTase are conserved in most cases. Most of the indolic compounds bearing the substituents shown in Figure 2 had little strain upon binding to the FTase ($<$6 kcal/mol). The SEED binding energies of the candidate ligands are more favorable than that of the minimized VIM tripeptide (Table 3). This is due to significantly better electrostatic interactions, while the other energy terms are comparable. The CHARMM binding energies, which do not include solvation, are comparable (Table 4). Although it is outside the scope of this study, it might be interesting to use a multi-layer scoring system as proposed by So and Karplus[55] to try to predict the binding affinity of the candidate ligands.

CONCLUSIONS

The comparison of the hydrophobicity maps of the unliganded and complexed FTase has revealed that the binding of FPP significantly increases the apolar character of the active site surface. The displacement of the Arg202β side chain upon binding of FPP is an example of induced fit in which the ligand modifies the electrostatic properties of the binding site. The program SEED was used to dock small- and medium-sized fragments into the region of the FTase active site where the CaaX motif binds. The SEED functionality maps are consistent with crystallographic data[31,43,44] and define two main features of potent peptidic ligands. The first is the need for a polar side chain at a1, which is in contrast with known mammalian sequence[1,17,51–53] but in accord with recent experimental results on combinatorial tetrapeptide libraries.[50] Furthermore, recent X-ray data indicate that the position of the Val side chain at a1 is not optimal and its orientation is completely different in a zinc-depleted FTase.[43] The second feature is the importance of aromatic side chains at position a2, which is in agreement with results obtained using a thin layer chromatography assay to define classes of peptidic inhibitors that are not farnesylated.[54]

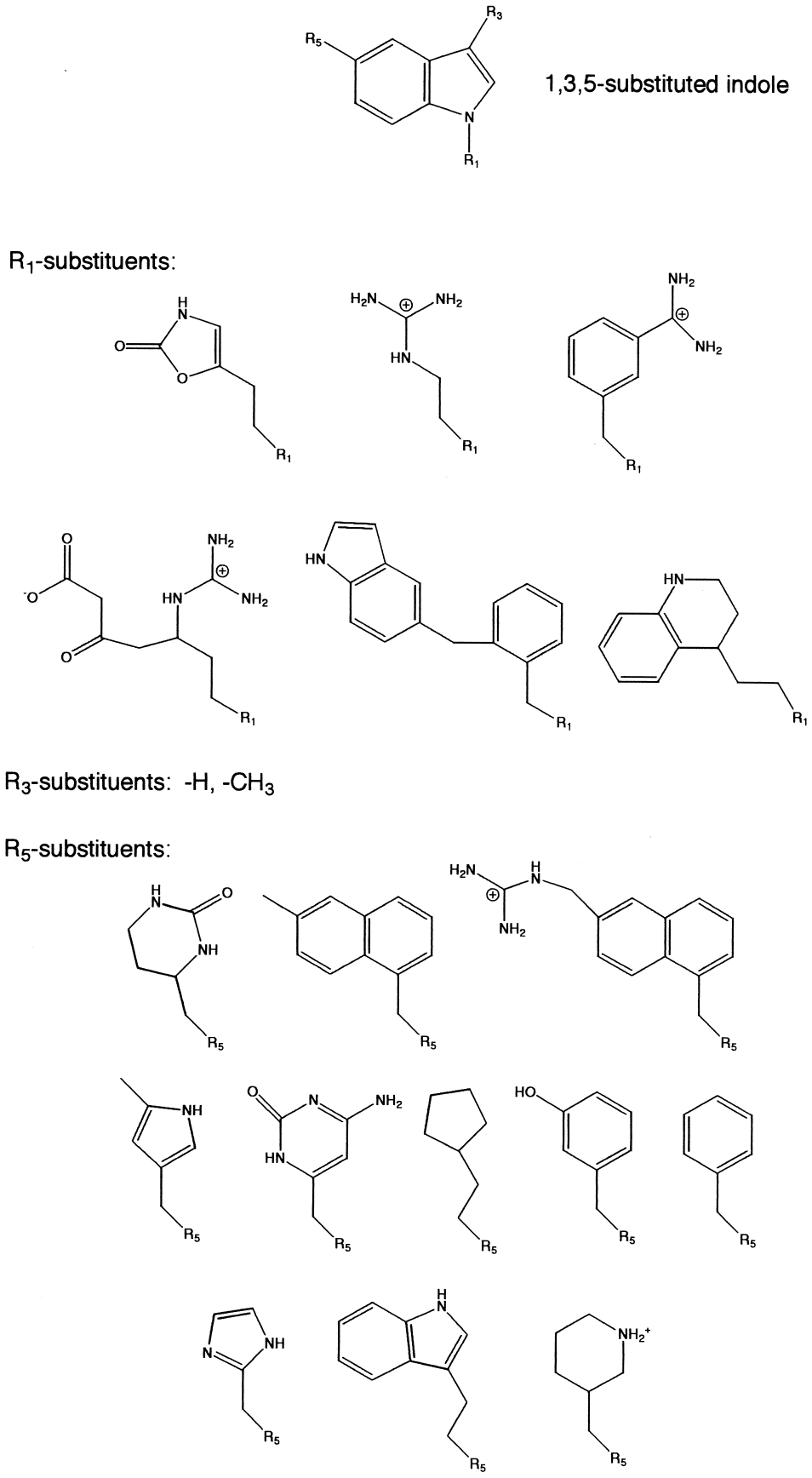

Figure 2. Library of indolic FTase inhibitors.

Table 3. SEED energies of the VIM peptide and four disubstituted indoles

		Intermolecular		Electrostatic desolvation	
	$\Delta G^{a}_{binding}$	vdWaals	Elect	Receptor	Ligand
VIM[b]	−7.7	−32.4	−0.9	16.5	7.1
Lig1	−17.8	−30.4	−29.3	16.8	25.1
Lig2	−17.0	−19.5	−38.5	17.4	23.6
Lig3	−17.2	−31.7	−10.1	16.7	7.9
Lig4	−13.2	−24.3	−14.1	17.9	7.3

All energy values are in kcal/mol.
[a] Sum of the values in the next four columns.
[b] The cystein was neglected to be consistent with the indolic compounds that do not contact the zinc atom.

Table 4. CHARMM energies of the VIM peptide and four disubstituted indoles

		Intermolecular			Ligand Strain			
	$\Delta G^{a}_{binding}$	Total[b]	vdWaals	Elect	Total[c]	vdWaals	Elect	Bonding
VIM[d]	−44.9	−48.2	−38.2	−10.0	3.3	0.2	−0.1	3.1
Lig1	−48.7	−54.6	−28.4	−26.2	5.9	0.9	3.1	2.0
Lig2	−43.4	−5.8	−22.9	−28.8	8.4	1.9	2.7	3.8
Lig3	−40.3	−45.9	−31.7	−14.2	5.6	1.5	1.0	3.1
Lig4	−39.1	−43.8	−26.3	−17.5	4.6	2.2	0.7	1.7

All energy values are in kcal/mol.
[a] Sum of the values of the total intermolecular interaction and the ligand strain.
[b] Sum of the values in the next two columns.
[c] Sum of the values in the next three columns.
[d] The cystein was neglected to be consistent with the indolic compounds that do not contact the zinc atom.

The detailed functionality maps presented in this paper, which are available in electronic format upon request, might facilitate the design of novel inhibitors of FTase as well as the optimization of known lead compounds.

A library of 1,3,5-substituted indoles was designed by using the SEED functionality maps as input for the program CCLD. Although both the SEED binding energies, which contain solvation, and the CHARMM energies of these candidate ligands are favorable, the validity and usefulness of the present indolic library have to await synthesis and measurements of inhibitory potency.

ACKNOWLEDGMENTS

We thank M. Scarsi, N. Budin, and C. Tenette-Souaille for helpful discussions and A. Widmer (Novartis Pharma Inc., Basel, Switzerland) for the molecular modelling program WITNOTP, which was used for visual analysis of the results and for preparing Figure and Color Plates 1 (bottom) to 5. Color Plate 1 (top) was made with GRASP.[37] This work was supported by the Cancer Society of the Canton Zürich, the Helmut Horten Foundation, and the Swiss National Science Foundation (grant no. 31-53604.98 to A.C.).

The program SEED (for SGI or PC running the Linux operating system) as well as the library of fragments (mol2 format) and the functionality maps of FTase are available for not-for-profit institutions from the corresponding author.

REFERENCES

1. Barbacid, M. Ras genes. *Ann. Rev. Biochem.* 1987, **56,** 779–827
2. Bos, J.L. Ras oncogenes in human cancer: a review. *Cancer Research* 1989, **49,** 4682–4689
3. Keely, P., Parise, L., and Juliano, R. Integrins and GTPases in tumour cell growth, motility and invasion. *Trends Cell Biol.* 1998, **8,** 101–106
4. Farnsworth, C.C., Wolda, S.L., Gelb, M.H., and Glomset, J.A. Human lamin B contains a farnesylated cysteine residue. *J. Biol. Chem.* 1989, **264,** 20422–20429
5. Casey, P.J., Solski, P.A., Der, C.J., and Buss, J.E. p21ras is modified by a farnesyl isoprenoid. *Proc. Nat. Acad. Sci. USA.* 1989, **86,** 8323–8327
6. Maltese,W.A., and Robishaw, J.D. Isoprenylation of C-terminal cysteine in a G-protein gamma subunit. *J. Biol. Chem.* 1990, **265,** 18071–18074
7. Maltese, W.A. Posttranslational modification of proteins by isoprenoids in mammalian cells. *FASEB J.* 1990, **4,** 3319–3328
8. Cox, A.D., and Der, C.J. Protein prenylation: more than just glue? *Curr. Opin. Cell Biol.* 1992, **4,** 1008–1016
9. Magee, A.I., Newman, C.M., Giannakouros, T., Hancock, J.F., Fawell, E., and Armstrong, J. Lipid modifications and function of the ras superfamily of proteins. *Biochem. Soc. Transact.* 1992, **20,** 497–499
10. Clarke, S. Protein isoprenylation and methylation at

carboxyl-terminal cysteine residues. *Ann. Rev. Biochem.* 1992, **61,** 355–386
11. Hudes, G., Schol, J., and Baab, J. Phase I clinical and pharmaco-kinetic trial of the farnesyltransferase inhibitor R115777 on a 21-day dosing schedule. *Proc. Am. Soc. Clin. Oncol.* 1999 (Abstract 601)
12. Adjei, A.A., Erlichman, C., and Davis, J.N. A phase I and pharmacologic study of the farnesyl protein transferase inhibitor SCH 66336 in patients with locally advanced or metastatic cancer. *Proceed Amer. Soc. Clin. Oncol.* 1999 (abstr 598)
13. Britten, C.D., Rowinsky, E., and Yao, S.L. The farnesyl protein transferase (FT-Pase) inhibitor L-778, 123 in patients with solid cancers. *Proc. Amer. Soc. Clin. Oncol.* 1999 (abstr 597)
14. Nagasu, T., Yoshimatsu, K., Rowell, C., Lewis, M.D., and Garcia, A.M. Inhibition of human tumor xenograft growth by treatment with the farnesyltransferase inhibitor B956. *Cancer Research* 1995, **55,** 5310–5314
15. Garcia, A.M., Rowell, C., Ackermann, K., Kowalczyk, J.J., and Lewis, M.D. Peptidomimetic inhibitors of Ras farnesylation and function in whole cells. *J. Biol. Chem.* 1993, **268,** 18415–18418
16. Furfine, E.S., Leban, J.J., Landavazo, A., Moomaw, J.F., and Casey, P.J. Protein farnesyltransferase: kinetics of farnesyl pyrophosphate binding and product release. *Biochem.* 1995, **34,** 6857–6862
17. Fukada, Y., Takao, T., Ohguro, H., Yoshizawa, T., Akino, T., and Shimonishi, Y. Farnesylated gamma-subunit of photoreceptor G protein indispensable for GTP-binding. *Nature* 1990, **346,** 658–660
18. Rowinsky, E.K., Windle, J.J., and Von Hoff, D.D. Ras protein farnesyltransferase: A strategic target for anticancer therapeutic development. *J. Clin. Oncol.* 1999, **17,** 3631–3652
19. Leonard, D.M. Ras farnesyltransferase: A new therapeutic target. *J. Med. Chem.* 1997, **40,** 2971–2990
20. Rarey, M., Kramer, B., Lengauer, T., and Klebe, G. A fast flexible docking method using an incremental construction algorithm. *J. Molec. Biol.* 1996, **261,** 470–489
21. Eldridge, M.D., Murray, C.W., Auton, T.R., Paolini, G.V., and Mee, R.P. Empirical scoring functions: I. The development of a fast empirical scoring function to estimate the binding affinity of ligands in receptor complexes. *J. Comp. Aided Mol. Des.* 1997, **11,** 425–445
22. Baxter, C.A., Murray, C.W., Clark, D.E., Westhead, D.R., and Eldridge, M.D. Flexible docking using Tabu search and an empirical estimate of binding affinity. *Proteins* 1998, **33,** 367–382
23. Jones, G., Willett, P., Glen, R.C., Leach, A.R., and Taylor, R. Development and validation of a genetic algorithm for flexible docking. *J. Molec. Biol.* 1997, **267,** 727–748
24. Lorber, D.M., and Shoichet, B.K. Flexible ligand docking using conformational ensembles. *Protein Sci.* 1998, **7,** 938–950
25. Miranker, A., and Karplus, M. Functionality maps of binding sites: a multiple copy simultaneous search method. *Proteins* 1991, **11,** 29–34
26. Majeux, N., Scarsi, M., Apostolakis, J., Ehrhardt, C., and Caflisch, A. Exhaustive docking of molecular fragments with electrostatic solvation. *Proteins* 1999, **37,** 88–105
27. Bemis, G.W., and Murcko, M.A. The properties of known drugs. 1. Molecular frameworks. *J. Med. Chem.* 1996, **39,** 2887–2893
28. Caflisch, A. Computational combinatorial ligand design: application to human alpha-thrombin. *J. Comp. Aided Mol. Des.* 1996, **10,** 372–396
29. Furka, A., and Bennett, W.D. Combinatorial libraries by portioning and mixing. *Combinatorial Chem. High Throughput Screening* 1999, **2,** 105–122
30. The Polyphor Catalogue of Core Structure 2000, Polyphor Ltd., CH-4123 Allschwil, Switzerland
31. Strickland, C.L., Windsor, W.T., Syto, R., Wang, L., Bond, R., Wu, Z., Schwartz, J., Le, H.V., Beese, L.S., and Weber, P.C. Crystal structure of farnesyl protein transferase complexed with a CaaX peptide and farnesyl diphosphate analogue. *Biochemistry* 1998, **37,** 16601–16611
32. Bernstein, F.C., Koetzle, T.F., Williams, G.J., Meyer Jr., E.E., Brice, M.D., Rodgers, J.R., Kennard, O., Shimanouchi, T., and Tasumi, M. The Protein Data Bank: a computer-based archival file for macromolecular structures. *J. Molec. Biol.* 1977, **112,** 535–542
33. Park, H.W., Boduluri, S.R., Moomaw, J.F., Casey, P.J., and Beese, L.S. Crystal structure of protein farnesyltransferase at 2.25 resolution. *Science* 1997, **275,** 1800–1804
34. Long, S.B., Casey, P.J., and Beese, L.S. Cocrystal structure of protein farnesyltransferase complexed with a farnesyl diphosphate substrate. *Biochemistry* 1998, **37,** 9612–9618
35. Brunger, A.T., and Karplus, M. Polar hydrogen positions in proteins: empirical energy placement and neutron diffraction comparison. *Proteins* 1988, **4,** 148–156
36. Brooks, B.R., Bruccoleri, R.E., Olafson, B.D., States, D.J., Swaminathan, S., and Karplus, M. CHARMM: a program for macromolecular energy, minimization, and dynamics calculations. *J. Comp. Chem.* 1983, **4,** 187–217
37. Nicholls, A., Sharp, K.A., and Honig, B. Protein folding and association: insights from the interfacial and thermodynamic properties of hydrocarbons. *Proteins* 1991, **11,** 281–296
38. Eisenhaber, F., and Argos, P. Hydrophobic regions on protein surfaces: definition based on hydration shell structure and a quick method for their computation. *Protein Engineer.* 1996, **9,** 1121–1133
39. Scarsi, M., Majeux, N., and Caflisch, A. Hydrophobicity at protein surfaces. *Proteins: Struct. Funct. Genet.* 1999, **37,** 565–575
40. Scarsi, M., Apostolakis, J., and Caflisch, A. Continuum electrostatic energies of macromolecules in aqueous solutions. *J. Phys. Chem. A.* 1997, **101,** 8098–8106
41. Scarsi, M., Apostolakis, J., and Caflisch, A. Comparison of a GB solvation model with explicit solvent simulations: potentials of mean force and conformational preferences of alanine dipeptide and 1,2-dichloroethane. *J. Phys. Chem. B.* 1998, **102,** 3637–3641
42. James, G.L., Goldstein, J.L., Brown, M.S., Rawson, T.E., Somers, T.C., McDowell, R.S., Crowley, C.W., Lucas, B.K., Levinson, A.D., and Masters, J.C. Benzodiazepine peptidomimetics—potent inhibitors of Ras farnesylation in animal cells. *Science* 1993, **260,** 1937–1942
43. Long, S.B., Casey, P.J., and Beese, L.S. The basis

forK-Ras4B binding specificity to protein farnesyltransferase revealed by 2 Å resolution ternary complex structures. *Structure* 2000, **8,** 209–222
44. Strickland, C.L., Weber, P.C., Windsor, W.T., Wu, Z., Le, H.V., Albanese, M.M., Alvarez, C.S., Cesarz, D., del Rosario, J., Deskus, J., Mallams, A.K., Njoroge, F.G., Piwinski, J.J., Remiszewski, S., Rossman, R.R., Taveras, A.G., Vibulbhan, B., Doll, R.J., Girijavallabhan, V.M., and Ganguly, A.K. Tricyclic farnesyl protein transferase inhibitors: crystallographic and calorimetric studies of structure-activity relationships. *J. Med. Chem.* 1999, **42,** 2125–2135
45. Omer, C.A., Kral, A.M., Diehl, R.E., Prendergast, G.C., Powers, S., Allen, C.M., Gibbs, J.B., and Kohl, N.E. Characterization of recombinant human farnesyl-protein transferase: cloning, expression, farnesyl diphosphate binding, and functional homology with yeast prenyl-protein transferase. *Biochemistry* 1993, **32,** 5167–5176
46. Moores, S.L., Schaber, M.D., Mosser, S.D., Rands, E., O'Hara, M.B., Garsky, V.M., Marschall, M.S., Pompliano, D.L., and Gibbs, J.B. Sequence dependence of protein isoprenylation. *J. Biol. Chem.* 1991, **266,** 14603–14610
47. Caplin, B.E., Hettich, L.A., and Marschall, M.S. Substrate characterization of the *Saccharomyces cerevisiae* protein farnesyltransferase and type-I protein geranylgeranyltransferase. *Biochim. Biophys. Acta* 1994, **1205,** 39–48
48. Zhang, F.L., Kirschmeier, P., Carr, D., James, L., Bond, R.W., Wang, L., Patton, R., Windsor, W.T., Syto, R., Zhang, R., and Bishop, W.R. Characterization of Haras, N-ras, Ki-Ras4A, and Ki-Ras4B as in vitro substrates for farnesyl protein transferase and geranylgeranyl protein transferase type I. *J. Biol. Chem.* 1997, **272,** 10232–10239
49. Reiss, Y., Stradley, S.J., Gierasch, L.M., Brown, M.S., and Goldstein, J.L. Sequence requirement for peptide recognition by rat brain p21ras protein farnesyltransferase. *Proc. Nat. Acad. Sci. USA* 1991, **88,** 732–736
50. Boutin, J.A., Marande, W., Petit, L., Loynel, A., Desmet, C., Canet, E., and Fauchere, J.L. Investigation of S-farnesyl transferase substrate specificity with combinatorial tetrapeptide libraries. *Cell. Signal.* 1999, **11,** 59–69
51. Schafer, W.R., Kim, R., Sterne, R., Thorner, J., Kim, S.H., and Rine, J. Genetic and pharmacological suppression of oncogenic mutations in ras genes of yeast and humans. *Science* 1989, **245,** 379–385
52. Casey, P.J. Protein lipidation in cell signaling. *Science* 1995, **268,** 221–225
53. Foster, R., Hu, K.Q., Lu, Y., Nolan, K.M., Thissen, J., and Settleman, J. Identification of a novel human Rho protein with unusual properties: GTPase deficiency and in vivo farnesylation. *Mol. Cell. Biol.* 1996, **16,** 2689–2699
54. Goldstein, J.L., Brown, M.S., Stradley, S.J., Reiss, Y., and Gierasch, L.M. Nonfarnesylated tetrapeptide inhibitors of protein farnesyltransferase. *J. Biol. Chem.* 1991, **266,** 15575–15578
55. So, S.-S., and Karplus, M. A comparative study of ligand-receptor complex binding affinity prediction methods based on glycogen phosphorylase inhibitors. *J. Comp. Aided Mol. Des.* 1999, **13,** 243–258